AGU PUBLICATIONS

Geophysical Research Letters

RESEARCH LETTER
10.1002/2016GL070457

Key Points:
- This is the first model intercomparison concerning climate change including Greenland melt and a probabilistic uncertainty assessment
- Impact of Greenland melt on future overturning circulation is small but nonnegligible especially for high-end global warming scenarios
- Likelihood of a full overturning collapse remains exceptionally small if global warming is limited to less than 5 K

Supporting Information:
- Supporting Information S1

Correspondence to:
P. Bakker,
pbakker@marum.de

Citation:
Bakker, P., et al. (2016), Fate of the Atlantic Meridional Overturning Circulation: Strong decline under continued warming and Greenland melting, *Geophys. Res. Lett.*, *43*, 12,252–12,260, doi:10.1002/2016GL070457.

Received 14 JUL 2016
Accepted 9 NOV 2016
Accepted article online 11 NOV 2016
Published online 13 DEC 2016

Fate of the Atlantic Meridional Overturning Circulation: Strong decline under continued warming and Greenland melting

P. Bakker[1,2], A. Schmittner[1], J. T. M. Lenaerts[3], A. Abe-Ouchi[4], D. Bi[5], M. R. van den Broeke[3], W.-L. Chan[4], A. Hu[6], R. L. Beadling[7], S. J. Marsland[5], S. H. Mernild[8,9], O. A. Saenko[10], D. Swingedouw[11], A. Sullivan[5], and J. Yin[7]

[1]College or Earth, Ocean, and Atmospheric Sciences, Oregon State University, Corvallis, Oregon, USA, [2]Now at MARUM, University of Bremen, Bremen, Germany, [3]Institute for Marine and Atmospheric research, Utrecht University, Utrecht, Netherlands, [4]Atmosphere and Ocean Research Institute, University of Tokyo, Tokyo, Japan, [5]CSIRO Oceans and Atmosphere, Aspendale, Victoria, Australia, [6]National Center for Atmospheric Research, Boulder, Colorado, USA, [7]Department of Geosciences, University of Arizona, Tucson, Arizona, USA, [8]Faculty of Engineering and Science, Sogn og Fjordane University College, Sogndal, Norway, [9]Antarctic and Sub-Antarctic Program, Universidad de Magallanes, Punta Arenas, Chile, [10]Canadian Centre for Climate Modelling and Analysis, Victoria, British Columbia, Canada, [11]Institut Pierre-Simon Laplace, Paris, France

Abstract The most recent Intergovernmental Panel on Climate Change assessment report concludes that the Atlantic Meridional Overturning Circulation (AMOC) could weaken substantially but is very unlikely to collapse in the 21st century. However, the assessment largely neglected Greenland Ice Sheet (GrIS) mass loss, lacked a comprehensive uncertainty analysis, and was limited to the 21st century. Here in a community effort, improved estimates of GrIS mass loss are included in multicentennial projections using eight state-of-the-science climate models, and an AMOC emulator is used to provide a probabilistic uncertainty assessment. We find that GrIS melting affects AMOC projections, even though it is of secondary importance. By years 2090–2100, the AMOC weakens by 18% [−3%, −34%; 90% probability] in an intermediate greenhouse-gas mitigation scenario and by 37% [−15%, −65%] under continued high emissions. Afterward, it stabilizes in the former but continues to decline in the latter to −74% [+4%, −100%] by 2290–2300, with a 44% likelihood of an AMOC collapse. This result suggests that an AMOC collapse can be avoided by CO_2 mitigation.

1. Introduction

Changes of the Atlantic Meridional Overturning Circulation (AMOC) strongly influence the distributions of heat, nutrients, and carbon in the ocean, thus affecting global climate, ecosystems, and biogeochemical cycles [*Ganachaud and Wunsch*, 2000; *Schmittner*, 2005]. The most recent Intergovernmental Panel on Climate Change (IPCC) assessment report [*Stocker et al.*, 2013] concludes that the AMOC will probably weaken but is very unlikely to collapse in the 21st century [*Schmittner et al.*, 2005; *Cheng et al.*, 2013; *Stocker et al.*, 2013; *Schleussner et al.*, 2014]. The Greenland Ice Sheet (GrIS) has been losing mass at increasing rates over recent decades, with observational mass loss estimates of $171 \pm 84\,\mathrm{Gt\,yr^{-1}}$ (~0.005 sverdrup (Sv); $1\,\mathrm{Sv} = 10^6\,\mathrm{m^3\,s^{-1}}$) and a trend of $-16.8 \pm 2.8\,\mathrm{Gt\,yr^{-2}}$ [*van den Broeke et al.*, 2016; over the period 1991–2015], and future GrIS mass loss is projected to increase further for centuries to come [*Fettweis et al.*, 2013; *Lenaerts et al.*, 2015]. However, future mass loss of the GrIS in previous comprehensive climate model simulations has been either neglected or highly idealized in terms of magnitude, spatial, and temporal characteristics; e.g., in the most recent model intercomparison, *Swingedouw et al.* [2015] released 0.1 Sv for 40 years uniformly around Greenland. Moreover, long-term AMOC projections are rare, and to our knowledge probabilistic AMOC projections are not available beyond 2100 [*Schleussner et al.*, 2014]. Here in a community-based effort, the AMOC Model Intercomparison Project (AMOCMIP), current best-estimates of GrIS mass loss are included in state-of-the-science, IPCC class, general circulation model (GCM) simulations up to the year 2300. Furthermore, we use a physics-based AMOC emulator [*Bakker and Schmittner*, 2016] tuned to the GCM results to provide a probabilistic assessment of the impacts of global warming and GrIS melt on the AMOC. This enables us for the first time to evaluate the impact of increased meltwater runoff from the GrIS on the future evolution of the AMOC on a multicentennial time scale and to quantify the likelihood of a future AMOC collapse.

Anthropogenic climate change might weaken the strength of the AMOC through enhanced poleward moisture transport, increased high-latitude precipitation and runoff [*Manabe and Stouffer*, 1999], changed surface heat fluxes [*Gregory et al*., 2005], and increased ice sheet meltwater discharge that stabilizes the water column in deep convection areas [*Manabe and Stouffer*, 1999; *Stouffer et al*., 2006]. Theories and models suggest that the AMOC may have two stable states [*Stommel*, 1961] and that crossing the stability thresholds can result in a rapid and irreversible circulation collapse [e.g., *Rahmstorf*, 1995]. Such a collapse, in realistic future climate change scenarios, is not shown by the majority of GCMs [*Stocker et al*., 2013; *Schleussner et al*., 2014], notwithstanding some exceptions [*Drijfhout et al*., 2015]. However, the probability of an AMOC collapse depends critically on uncertain model-dependent factors such as the stability of the AMOC, the magnitude of regional warming, changes in the hydrological cycle, and GrIS mass loss. The resulting uncertainty space is large and cannot be fully covered with the limited number of existing GCM simulations. Here we use an efficient tool to emulate the response of complex GCMs in order to sample a much wider range of uncertainty space to provide a comprehensive probabilistic assessment of future AMOC weakening that is necessary for an improved risk assessment by policy makers.

2. Materials and Methods

2.1. AMOCMIP Climate Models

A total of eight state-of-the-science GCMs participated in AMOCMIP (ACCESS1.0 [*Dix et al*., 2013], CanESM2 [*Yang and Saenko*, 2012], CCSM4 [*Meehl et al*., 2012], CESM1.1.2 [*Meehl et al*., 2013], GFDL-ESM2Mb [*Dunne et al*., 2012], IPSL-CM5A-LR [*Dufresne et al*., 2013], MIROC4m [*Hasumi and Emori*, 2004], and OSUVic [*Schmittner et al*., 2011]) and generated 21 individual climate projections that include improved GrIS mass loss estimates for two global warming scenarios (Representative Concentration Pathway RCP4.5 and RCP8.5) [*Meinshausen et al*., 2011], the former representing an intermediate greenhouse-gas mitigation scenario and the latter a scenario with continued high greenhouse-gas emissions. Each model performed at least one RCP experiment up to the year 2100 including GrIS mass loss, but most performed more and longer experiments (Table S1 in the supporting information). The AMOCMIP simulations are supplemented with existing historical, RCP4.5, and RCP8.5 simulations that do not include GrIS mass loss. Throughout this study, the maximum overturning stream function at 26°N below 500 m depth is taken as a measure of the AMOC strength in accordance with observations [RAPID; *McCarthy et al*., 2015].

2.2. GrIS Meltwater Forcing

In AMOCMIP we follow the methodology of *Lenaerts et al*. [2015] to construct temporally and spatially varying GrIS meltwater forcings. The method prescribes a strong relation between local midtropospheric summer temperatures and annual mean runoff for eight different sections of the GrIS, based on RACMO2 high-resolution (~11 km) regional climate model simulations. RACMO2 simulations were run for the period 1971–2100 and forced at the boundaries by HadGEM2-ES GCM output under the RCP4.5 scenario [*Lenaerts et al*., 2015]. Strong spatial variations in GrIS runoff are included by performing these calculations separately over eight glacial drainage sections [*Wouters et al*., 2008]. A fixed seasonal GrIS runoff cycle is imposed based on a scaling of the average RACMO2 seasonal cycle for the period 1960–2012.

To derive GrIS mass loss projections for AMOCMIP, we combine the relations described by *Lenaerts et al*. [2015] with CMIP5 multimodel mean (MMM) midtropospheric summer temperature anomalies. These anomalies are calculated from all available RCP4.5 and RCP8.5 simulations that cover (part of) the period 2006–2300, using only a single ensemble member if multiple ones exist. Because of data availability, the MMM temperature anomalies consist of from 39 to as little as 5 model simulations for individual scenarios and time intervals. Temperature anomalies are calculated with respect to the GCM's historical average 1971–2000 temperatures. The GrIS runoff parameterization includes changes in precipitation, evaporation, snow and ice melt, and meltwater refreezing and retention in the snowpack [*Lenaerts et al*., 2015]. The high complexity and resolution of RACMO2 compared to GCMs ensures a much better representation of real-world atmospheric and snow processes and topography.

Not considered in the AMOCMIP GrIS mass loss projections are changes in solid ice discharge (iceberg calving). Presently, the constraints on the sign and magnitude of GrIS solid-ice discharge projections are insufficient to be included in the AMOCMIP forcing [*Lenaerts et al*., 2015; *Nick et al*., 2009]. To assess the potential role of future changes in solid ice discharge, a set of additional experiments is performed with the AMOC emulator (see supporting information Text S1). The above described GrIS mass loss projections are added to

two different historical GrIS runoff "baselines": the amount of historical GrIS runoff, including a spatial pattern and a seasonal cycle. A first one (gGrISmelt) based on the 1971–2000 average for the individual GCMs and a second one (rGrISmelt) that is a combination of RACMO2-based historical (1971–2000) liquid runoff and observed GrIS solid ice calving rate [*Enderlin et al*., 2014] that is spatially distributed over the North Atlantic and Arctic based on a high-resolution ocean-iceberg simulation [*van den Berk and Drijfhout*, 2014]. Including these two different GrIS runoff baselines allows us to assess the importance of GCM biases in present-day GrIS discharge. The forcing protocol of the AMOCMIP climate change projection allows, for the first time, a model intercomparison of the combined effects of global warming and GrIS mass loss on AMOC evolution and the climate in general. More details are available in Text S1.

2.3. Uncertainty Analysis

The 21 AMOCMIP GCM simulations present an important improvement over previous attempts [e.g., *Swingedouw et al*., 2015] because of the number of different GCMs that was used, the more realistic forcing scenarios that were considered and because they provide projections up to the year 2300. Still, they only sample a limited portion of the full uncertainty space. An AMOC emulator is used here to extend the sampled uncertainty range and provide a more comprehensive probabilistic assessment. The AMOC emulator is a four-box model following *Stommel* [1961] and *Zickfeld et al*. [2004] that uses physical and dynamical relationships to represent the most important mechanisms and feedbacks that govern the AMOC's response to changes in surface temperatures and freshwater input [*Bakker and Schmittner*, 2016]. The AMOC emulator can reproduce the behavior of a specific GCM by optimizing a number of free parameters through simulated annealing [*Lombardi*, 2015] such that the difference between the AMOC's response in the GCM and the AMOC emulator to a given set of changes in boundary conditions is minimized. Tuning of the AMOC emulators for each of the GCM's is based on all performed AMOCMIP experiments and corresponding standard RCP scenarios, the total number of which differs per GCM. The parameter tuning procedure is repeated until for every GCM a total of 100 reasonable AMOC emulators are found, of which the 10 best are included in the Monte Carlo sampling. The performance of the AMOC emulator to mimic the original GCM-based AMOC projections is shown in Figure S1. An extensive description of the AMOC emulator, the free parameters, tuning procedure, and GCM-based AMOC emulator forcings as well as an evaluation of the predictive power of the AMOC emulator can be found elsewhere [*Bakker and Schmittner*, 2016]. The AMOC emulator enables the large numbers of simulations necessary to assess the full uncertainty of AMOC projections.

Five types of uncertainty are included in the probabilistic AMOC projections: greenhouse-gas concentration changes (GHG), climate sensitivity to GHG forcing including regional temperature changes (e.g., polar amplification), GrIS mass loss, and AMOC sensitivity to climate and GrIS meltwater forcing. These uncertainties are included using a Monte Carlo approach with a total of 10,000 samples per RCP scenario and set of forcings. In addition to these types of uncertainty, we approximate the error that is introduced by using an AMOC emulator rather than a GCM. GHG concentration changes are considered by using two different RCP scenarios (RCP4.5 and RCP8.5). The uncertainty in the AMOC's sensitivity to changes in regional temperatures and freshwater budgets is included by randomly picking one of the 80 AMOC emulator parameter sets that are tuned toward one of the participating GCMs. The uncertainty in climate sensitivity and regional temperature changes is treated simultaneously by semirandom sampling of CMIP5-based multimodel regional and global temperature change distributions for the period 2006–2300. Semirandom sampling, takes into account spatial correlations of temperature change that exist in the GCMs by using average regional temperatures over the last 10 years of all individual CMIP5 simulations for RCP4.5 and RCP8.5. The resulting correlations were then used in the semirandom sampling using Cholesky decomposition. This procedure captures uncertainties in climate sensitivity, polar amplification, and regional temperature change differences while maintaining a realistic degree of regional correlation. Finally, GrIS mass loss uncertainty is included by a combination of (1) semirandom sampling of midtropospheric summer temperature changes over Greenland following the method described above and (2) a random sampling of the uncertainty in the calculated second-order polynomial relations derived by recalculating them on random 95% subsamples of the original data [*Lenaerts et al*., 2015]. The resulting sampled ranges of regional temperatures and GrIS mass loss included in the probabilistic AMOC projections are shown in Figures S2 and S3. In addition to these uncertainties, we consider the error that is introduced by using the AMOC emulator to approximate the response of the GCMs. This error is based on an approximation of the mean and standard deviation of all combined GCM-to-AMOC emulator differences and added to all AMOC emulator simulations (see supporting information for more details).

3. AMOC Projections

3.1. AMOCMIP Results

For the first decade (2006–2016) the simulated maximum AMOC strength at 26°N differs substantially between GCMs, but the multimodel mean of 16.5 ± 3.0 Sv ($\mu \pm 1\sigma$) is consistent with the observed mean magnitude of 17.2 ± 2.2 Sv (1σ of interannual variability for period 2004–2014) [*McCarthy et al.*, 2015] (Figure 1). The simulated AMOC projections indicate similarities, but also significant intermodel differences, both in terms of AMOC weakening as well as AMOC sensitivity to GrIS meltwater. For RCP4.5 all models show a weakening until about year 2100 followed by a stabilization or recovery. By the year 2300 the AMOC has resumed its present-day strength in two models, while four show a sustained weakening of ~20–40%. Both the ACCESS1.0 and IPSL-CM5A-LR simulations show a substantial impact of increased GrIS meltwater in RCP4.5, almost doubling the AMOC weakening compared to the simulations with only global warming. For RCP8.5 all models indicate stronger and longer AMOC weakening compared with RCP4.5 and no significant recovery until year 2300, but the magnitude differs between models.

3.2. Probabilistic AMOC Projections

The results for the intermediate GHG mitigation scenario RCP4.5 indicate an AMOC weakening of 18% by years 2090–2100 (median; compared to 2006) with 3–34% for the 90–100% probability interval and a stabilization after that (Figure 2). In the continued high greenhouse-gas emission scenario RCP8.5, the AMOC weakens by 37% [−15%, −65%] in years 2090–2100 and by 74% in years 2290–2300, albeit with a large 90–100% probability interval from a 4% strengthening to a 100% weakening. The presented values for the years 2090–2100 are similar to previous probabilistic estimates [*Schleussner et al.*, 2014], providing confidence in the applied methodology. The mean of the GCM-based AMOC projections shows a similar evolution albeit a somewhat larger decrease compared with the AMOC emulator-based median (black and red lines in Figure 2, respectively). However, it is important to realize that the two means are not expected to overlap. This is because the number of models included in the GCM-based mean differs per scenario (RCP4.5 versus RCP8.5) and per time step. On the contrary, the AMOC emulator-based median effectively uses the available GCM scenarios to extrapolate and fill all missing data for all participating GCMs. Moreover, the relatively small AMOCMIP ensemble may be biased relative to the larger CMIP5 ensemble that is used in the forcing of the emulator.

The single forcing simulations show that both in the GCMs and the AMOC emulator the warming-induced AMOC weakening dominates over the GrIS meltwater impact (Figure 2). Nonetheless, the effect of increased GrIS mass loss is nonnegligible and induces an additional median AMOC weakening of about 37% in the years 2290–2300 in RCP8.5. Moreover, in the AMOC emulator the effects of increased GrIS mass loss are largest during the latter half of the projections, since GHG forcing alone leads to a stabilization of the AMOC during the 23rd century, but the simulation including GrIS mass loss shows a continuing decline until year 2300. The latter appears to be in contradiction with the GCM results that show only very little impact of GrIS mass loss in RCP8.5 (Figures 1 and 2); however, a RCP8.5 simulation with the apparently most sensitive GCM (IPSL-CM5A-LR) is not available for the GCM-based mean, thus partly explaining the mismatch. Probabilities for an AMOC collapse in years 2290–2300, defined here as a 90% reduction of its strength, increase from 20% to 44% when GrIS mass loss is included. These results are generally consistent with previous uncoordinated single-model GrIS mass loss experiments that suggest that the impact of increased GrIS melting is small for rates below ~0.1 Sv [*Fichefet et al.*, 2003; *Hu et al.*, 2009; *van den Berk and Drijfhout*, 2014; *Swingedouw et al.*, 2015].

In the GCM AMOCMIP experiments, future changes in GrIS solid ice discharge are neglected. We have performed idealized experiments with the AMOC emulator imposing $\pm 1\%\,\mathrm{yr}^{-1}$ changes of the observed value of ~0.016 Sv yr^{-1} [*van den Broeke et al.*, 2016] to investigate the impact of such high-end solid ice discharge changes, high-end since they translate into a doubling or complete cessation of GrIS solid ice discharge within the next ~70 years (see supporting information for details). The simulated impact of these high-end GrIS solid ice discharge experiments is an increase (decrease) of the AMOC weakening for more (less) solid ice discharge (Table S2). The impact of increased solid ice discharge is larger than that of a decrease of the same magnitude, which illustrates nonlinearities in the system. The largest effect is seen for increased solid ice discharge in scenario RCP8.5 at year 2300, where the AMOC is decreased by 91% compared to 74%

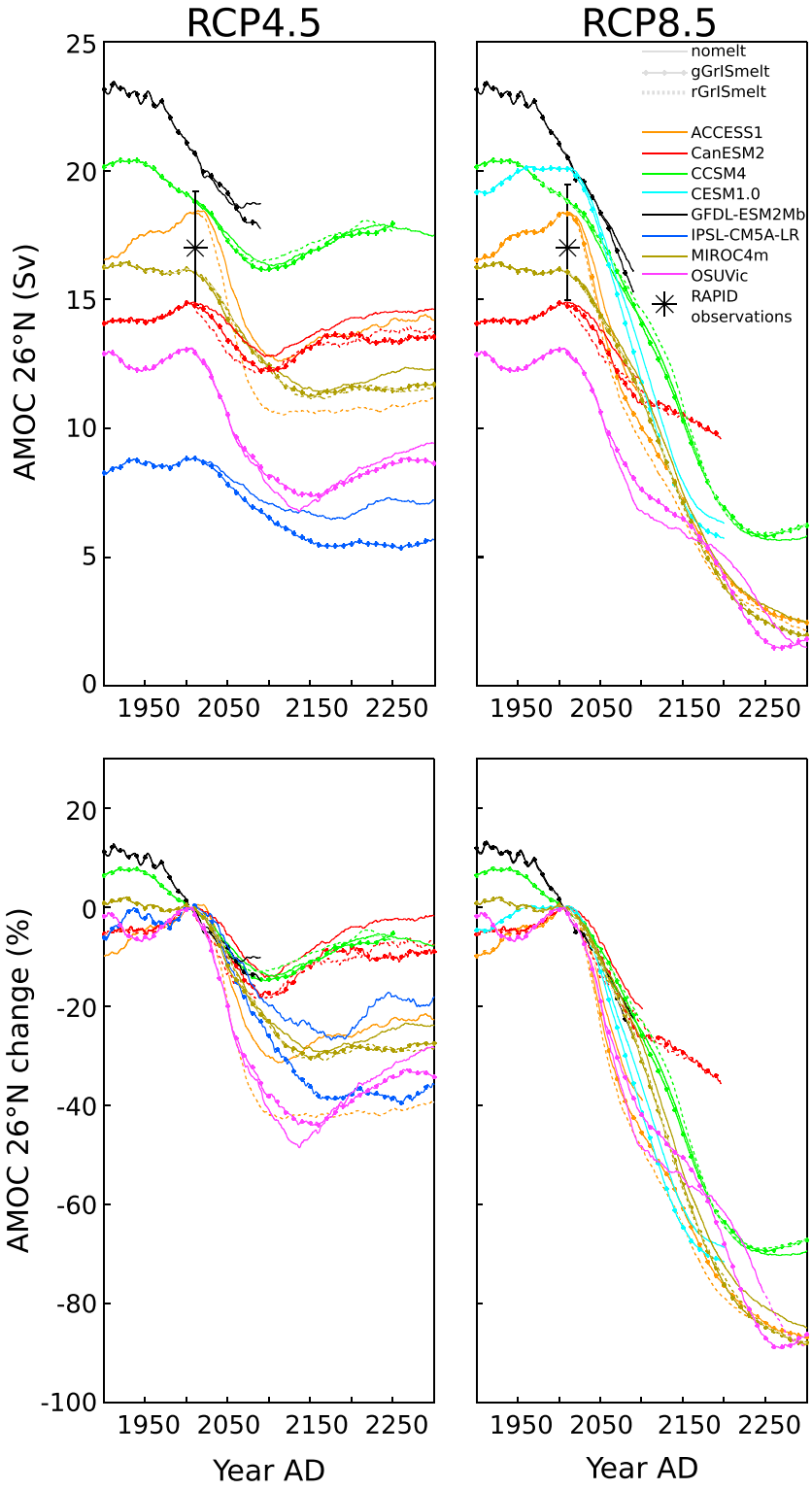

Figure 1. Simulated AMOC projections as part of AMOCMIP project. Results of eight GCMs are shown for the historical period combined with (left column) RCP4.5 and (right column) RCP8.5 and for the experiments without GrIS mass loss, with gGrISmelt and with rGrISmelt. Results are given for AMOC strength at 26°N (below 500 m; (top row) Sv) and for (bottom row) changes (%) in the AMOC strength at 26°N relative to 2006. A 50 year running mean is applied. Depicted RAPID data are an average over all available data between 2004 and 2014 [*McCarthy et al.*, 2015], with uncertainty bars reflecting the year-to-year variability ($1\sigma = 2.2$ Sv).

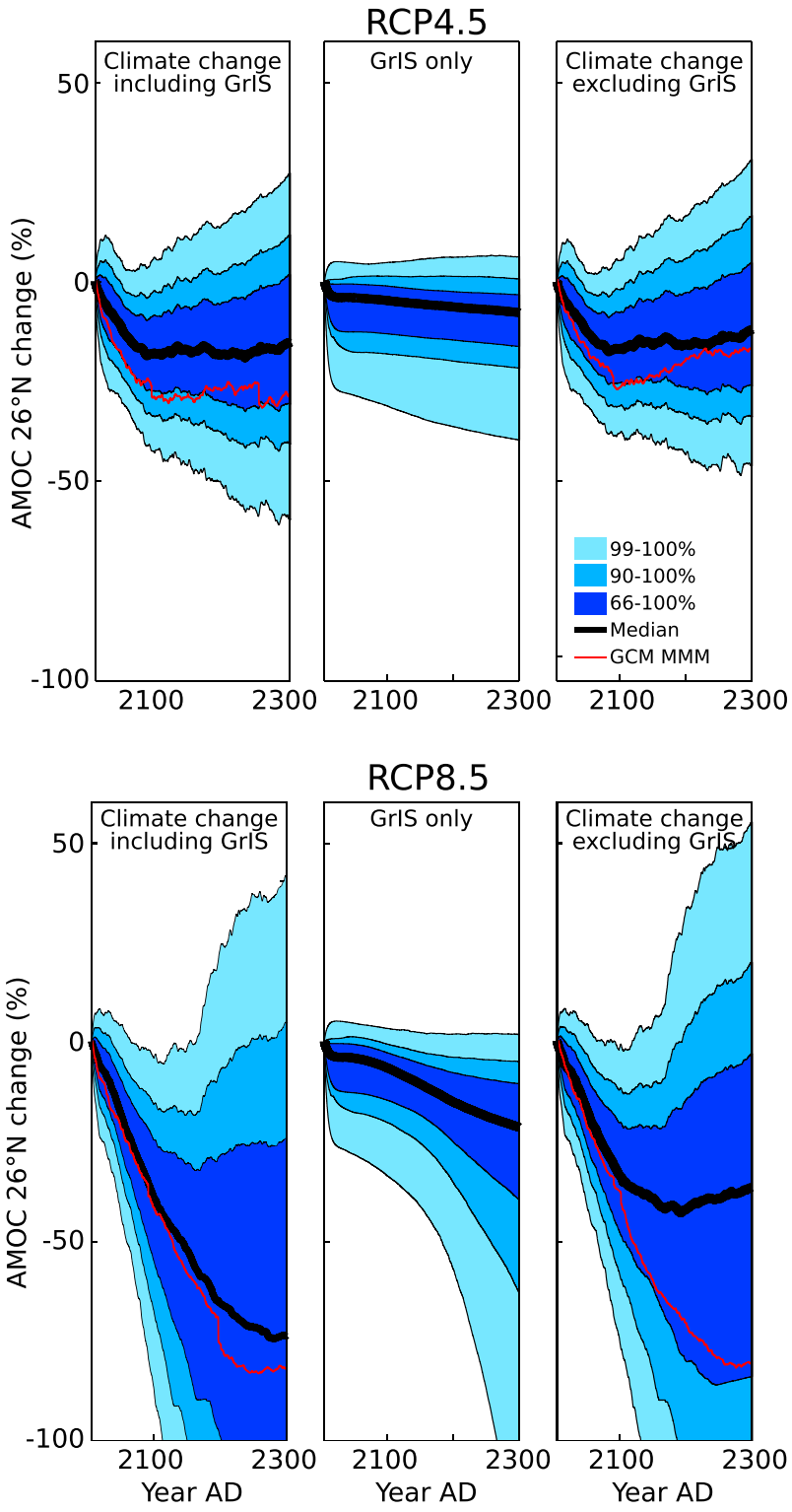

Figure 2. Probabilistic AMOC projections for RCP4.5 and RCP8.5 and impact of individual forcings. AMOC strength changes at 26°N (below 500 m; %) showing (from left to right) the combined impact of increasing temperatures and GrIS mass loss (Climate change including GrIS), GrIS mass loss only (GrIS only) and increasing temperatures only (Climate change excluding GrIS). Results are given for the median and three different confidence intervals (black line and blue shadings, respectively). Also indicated are the multimodel means over the AMOC evolution simulated by the GCMs (red line labeled GCM MMM; averaged over gGrISmelt and rGrISmelt if both exist). Note that the number of models used in the average differs over time and scenario.

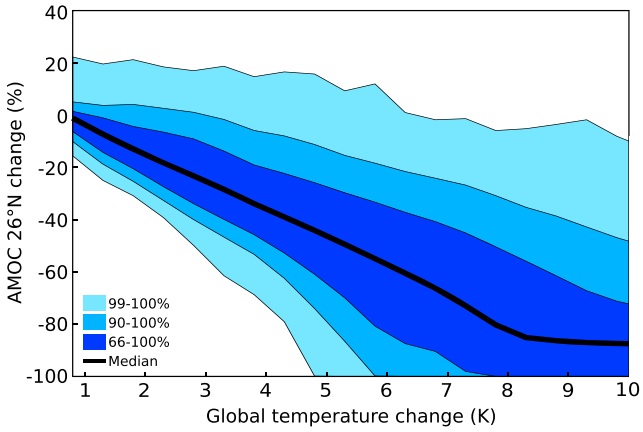

Figure 3. AMOC strength changes for changes in global temperature. Probabilistic assessment of annual mean AMOC strength changes at 26°N (below 500 m; %) as a function of global temperature change (K; relative to preindustrial). Results from 10.000 RCP4.5 and 10.000 RCP8.5 experiments are combined, spanning a large range of global temperature changes (Figure S2). Note that annual mean AMOC strength changes are not equilibrium values per se.

without changes in solid ice discharge. We stress that while these numbers give an impression of the potential importance of future changes in GrIS solid ice discharge, more constraints are required before its effect on future AMOC projections can be fully incorporated.

A more direct connection between the AMOC projections and risk assessments of global climate change can be made by examining yearly AMOC weakening values with respect to the period 1971–2005 as a function of global temperature change (Figure 3). This shows that for a global warming of 2 K above preindustrial levels, often presented as the safe limit, the AMOC is projected to weaken by 15% (90–100% probability interval of 3% strengthening to 28% weakening), and the probability of an AMOC collapse is negligible. This is contrary to a recent modeling study [*Hansen et al*., 2016] that used a much larger, and in our assessment unrealistic, Northern Hemisphere freshwater forcing (~0.1–0.25 Sv versus ~1–4 Sv, respectively) and finds a substantially larger probability of an AMOC collapse. According to our probabilistic assessment, the likelihood of an AMOC collapse remains very small (<1% probability) if global warming is below ~5 K relative to preindustrial, comparable to cumulative anthropogenic carbon emissions of ~2810 Gt C (using a linear scaling to global temperature change of 0.0016 K/Gt C) [*Stocker et al*., 2013]. Probabilities increase for greater global warming (11% for 6 K, 19% at 7 K, and 30% at 8 K; Figure 3). Including changes in GrIS solid ice discharge into our assessment only has limited impact on the calculated AMOC collapse probabilities. Whereas the influence of decreases in solid ice discharge is negligible, enhanced rates could increase the likelihood of an AMOC collapse by ~2–22% for global warming of 5–8 K (Figure S5).

4. Concluding Remarks

The use of an AMOC emulator has enabled a probabilistic assessment of the most important uncertainties of AMOC projections but also introduced a new source of uncertainty related to the simplified nature of the AMOC emulator compared to GCMs [*Bakker and Schmittner*, 2016]. The AMOC emulator has difficulties to simulate the AMOC recovery during the latter part of the RCP4.5 scenario that is found in some of the GCMs, and the AMOC emulator suggests a too large impact of GrIS melt, particularly during the 23rd century (Figure S1). It remains to be seen whether the differences in the mean AMOC weakening projected by the GCMs and AMOC emulator are an artifact of the AMOC emulator or the result of the fact that not all GCMs participating in AMOCMIP performed all scenarios for the entire period of interest.

In the design of AMOCMIP, possible mass loss of the Antarctic Ice Sheet has been neglected. Observations over the last two decades show that its contribution to present-day sea level rise is substantial (about 2/3 of GrIS contribution) [*Rignot et al*., 2011], but the future contribution remains highly uncertain. An investigation of the impact of combined GrIS and Antarctic Ice Sheet mass loss on the global ocean circulation would be an important next step to improve AMOC projections and more generally projections of the effects of future ice sheet mass loss on climate and ecosystems. The fact that the GCMs participating in AMOCMIP are not eddy resolving potentially impacts the robustness of our results. Recent studies have shown that if there is a significant impact at all, it is that coarser resolution GCMs slightly overestimate the sensitivity of the AMOC to GrIS melt relative to eddy resolving models [*Weijer et al*., 2012], implying a possible overestimation in our study of the impact of GrIS mass loss in forcing future AMOC changes. We only presented a first-order assessment of the impact of changes in the GrIS solid ice discharge rate on the AMOC strength. For

better constraints, detailed ice-sheet modeling studies are required, as well as GCM simulations that resolve the movement and melting of icebergs.

Notwithstanding the uncertainties and limitations listed in this manuscript, the AMOCMIP results combined with an extensive uncertainty analysis represent significant progress compared to previous AMOC projections. Our results show that by year 2090–2100, AMOC weakens by 18% in the median [−3%, −34%; 90–100% confidence interval] in the intermediate GHG mitigation scenario RCP4.5 in comparison to the twentieth century and about 37% [−15%, −65%] in the continued high greenhouse-gas emission scenario RCP8.5. In the latter this decline continues, eventually weakening by 74% [4%, −100%] in years 2290–2300. The impact of GrIS mass loss on the AMOC strength is smaller than the effects of projected climate warming and changes in the atmospheric hydrological cycle. However, it is nonnegligible it is nonnegligible and significantly increases AMOC weakening in both GCMs and the emulator, as well as the probabilities of an AMOC collapse under continued high greenhouse-gas emissions, particularly during the 23rd century and presumably beyond. However, our results suggest that if, by mitigation measures, CO_2 levels are kept well below those projected by the business-as-usual RCP8.5 scenario, the effect of GrIS mass loss on the AMOC strength will likely remain limited and an AMOC collapse, and its potentially dangerous impacts, is very unlikely.

Acknowledgments

P.B. and A.S. are supported by a grant from the National Oceanographic and Atmospheric Administration (award NA15OAR4310239). J.T.M.L. and M.R.v.d. B. acknowledge funding from the Netherlands Earth System Science Center (NESSC) and the Polar Program of the Netherlands Organization for Scientific Research (NWO). A.H. is supported by the Regional and Global Climate Modelling Program (RGCM) of the U.S. Department of Energy's Office of Science (BER), Cooperative Agreement DE-FC02-97ER62402 and simulations used the National Energy Research Scientific Computing Center which is supported by the Office of Science of the U.S. Department of Energy. O.A.S. thanks Warren Lee for his help with CanESM2 runs. Warren Lee for his help with CanESM2 runs. A.A. and W.C. are supported by the ArCS (conducted by the Ministry of Education, Culture, Sports,Science and Technology of the Japanese Government) and ICA-RUS (strategic R&D Area Project of the Environment Research and Technology Development Fund), used the JAMSTEC Earth Simulator, and thank the advice of M. Yoshimori and R. Ohgatio. Data from the RAPID MOC monitoring project are funded by the Natural Environment Research Council and are freely available from www.rapid.ac.uk/rapid-moc. Model output part of the AMOCMIP project will become available through ESGF (https://www.earthsystemcog.org/projects/amocmip/). The authors thank the Editor and two anonymous reviewers for their constructive comments.

References

Bakker, P., and A. Schmittner (2016), AMOC emulator for uncertainty assessment of future projections, *Geosci. Model Dev. Discuss*, doi:10.5194/gmd-2016-79.

Cheng, W., J. C. H. Chiang, and D. Zhang (2013), Atlantic Meridional Overturning Circulation (AMOC) in CMIP5 Models: RCP and historical simulations, *J. Clim.*, *26*(18), 7187–7197, doi:10.1175/JCLI-D-12-00496.1.

Dix, M., P. Vohralik, D. Bi, H. Rashid, and S. Marsland (2013), The ACCESS coupled model: Documentation of core CMIP5 simulations and initial results, *Aust. Meteorol. Oceanogr. J.*, *63*, 83–99.

Drijfhout, S., S. Bathiany, C. Beaulieu, V. Brovkin, M. Claussen, C. Huntingford, M. Scheffer, G. Sgubin, and D. Swingedouw (2015), Catalogue of abrupt shifts in Intergovernmental Panel on Climate Change climate models, *Proc. Natl. Acad. Sci. U.S.A.*, *112*(43), E5777–E5786, doi:10.1073/pnas.1511451112.

Dufresne, J.-L., M.-A. Foujols, S. Denvil, A. Caubel, and O. Marti (2013), Climate change projections using the IPSL-CM5 Earth System Model: From CMIP3 to CMIP5, *Clim. Dyn.*, *40*, 2123–2165, doi:10.1007/s00382-012-1636-1.

Dunne, J. P., G. J. John, A. J. Adcroft, S. M. Griffies, and R. W. Hallberg (2012), GFDL's ESM2 coupled climate-carbon Earth System Models Part 1: Physical formulation and baseline simulation characteristics, *J. Clim.*, *25*, 6646–6665, doi:10.1175/JCLI-D-11-00560.1.

Enderlin, E. M., I. M. Howat, S. Jeong, M. J. Noh, J. H. van Angelen, and M. R. van den Broeke (2014), An improved mass budget for the Greenland ice sheet, *Geophys. Res. Lett.*, *41*, 866–872, doi:10.1002/2013GL059010.

Fettweis, X., B. Franco, M. Tedesco, J. H. van Angelen, J. T. M. Lenaerts, M. R. van den Broeke, H. Gallée, J. H. van Angelen, and H. Gall (2013), Estimating the Greenland ice sheet surface mass balance contribution to future sea level rise using the regional atmospheric climate model MAR, *Cryosphere*, *7*, 289–469, doi:10.5194/tc-7-469-2013.

Fichefet, T., C. Poncin, H. Goosse, P. Huybrechts, I. Janssens, and H. Le Treut (2003), Implications of changes in freshwater flux from the Greenland ice sheet for the climate of the 21st century, *Geophys. Res. Lett.*, *30*(17), 1911, doi:10.1029/2003GL017826.

Ganachaud, A., and C. Wunsch (2000), Improved estimates of global ocean circulation, heat transport and mixing from hydrographic data, *Nature*, *408*, 453–458, doi:10.1038/35044048.

Gregory, J. M., et al. (2005), A model intercomparison of changes in the Atlantic thermohaline circulation in response to increasing atmospheric CO2 concentration, *Geophys. Res. Lett.*, *32*, L12703, doi:10.1029/2005GL023209.

Hansen, J., et al. (2016), Ice melt, sea level rise and superstorms: Evidence from paleoclimate data, climate modeling, and modern observations that 2°C global warming is highly dangerous, *Atmos. Chem. Phys.*, *16*, 3761–3812, doi:10.5194/acp-16-3761-2016.

Hasumi, H., and E. Emori (2004), K-1 coupled GCM (MIROC) description, K-1 Technical Report, CCSR/NIES/FRCGC.

Hu, A., G. A. Meehl, W. Han, and J. Yin (2009), Transient response of the MOC and climate to potential melting of the Greenland Ice Sheet in the 21st century, *Geophys. Res. Lett.*, *36*, L10707, doi:10.1029/2009GL037998.

Lenaerts, J. T. M., D. le Bars, L. van Kampenhout, M. Vizcaíno, E. M. Enderlin, and M. R. van den Broeke (2015), Representing Greenland ice sheet freshwater fluxes in climate models, *Geophys. Res. Lett.*, *42*, 6373–6381, doi:10.1002/2015GL064738.

Lombardi, A. M. (2015), Estimation of the parameters of ETAS models by simulated annealing, *Sci. Rep.*, *5*(8417), 1–11, doi:10.1038/srep08417.

Manabe, S., and R. J. Stouffer (1999), The role of thermohaline circulation in climate, *Tellus, Ser. A Dyn. Meteorol. Oceanogr.*, *51*(1 SPEC. ISS), 91–109, doi:10.1034/j.1600-0889.1999.00008.x.

McCarthy, G. D., D. A. Smeed, W. E. Johns, E. Frajka-Williams, B. I. Moat, D. Rayner, M. O. Baringer, C. S. Meinen, J. Collins, and H. L. Bryden (2015), Measuring the Atlantic Meridional Overturning Circulation at 26°N, *Prog. Oceanogr.*, *130*, 91–111, doi:10.1016/j.pocean.2014.10.006.

Meehl, G. A., et al. (2012), Climate system response to external forcings and climate change projections in CCSM4, *J. Clim.*, *25*, 3661–3683, doi:10.1175/JCLI-D-11-00240.1.

Meehl, G. A., W. M. Washington, J. M. Arblaster, A. Hu, H. Teng, J. E. Kay, A. Gettelman, D. M. Lawrence, B. M. Sanderson, and W. G. Strand (2013), Climate change projections in CESM1(CAM5) compared to CCSM4, *J. Clim.*, *26*, 6287–6308, doi:10.1175/JCLI-D-12-00572.1.

Meinshausen, M., et al. (2011), The RCP greenhouse gas concentrations and their extensions from 1765 to 2300, *Clim. Change*, *109*(1–2), 213–241, doi:10.1007/s10584-011-0156-z.

Nick, F. M., A. Vieli, I. M. Howat, and I. R. Joughin (2009), Large-scale changes in Greenland outlet glacier dynamics triggered at the terminus, *Nat. Geosci.*, *2*(2), 110–114, doi:10.1038/ngeo394.

Rahmstorf, S. (1995), Bifurcation of the Atlantic thermohaline circulation in response to changes in the hydrological cycle, *Nature*, *378*, 145–149, doi:10.1038/379847b0.

Rignot, E., I. Velicogna, M. R. van den Broeke, A. Monaghan, J. T. M. Lenaerts, E. Rignot, and I. Velicogna (2011), Acceleration of the contribution of the Greenland and Antarctic ice sheets to sea level rise, *Geophys. Res. Lett.*, *38*, L05503, doi:10.1029/2011GL046583.

Schleussner, C., A. Levermann, and M. Meinshausen (2014), Probabilistic projections of the Atlantic overturning, *Clim. Change*, *127*(3), 579–586, doi:10.1007/s10584-014-1265-2.

Schmittner, A. (2005), Decline of the marine ecosystem caused by a reduction in the Atlantic overturning circulation, *Nature*, *434*(7033), 628–633, doi:10.1038/nature03476.

Schmittner, A., M. Latif, and B. Schneider (2005), Model projections of the North Atlantic thermohaline circulation for the 21st century assessed by observations, *Geophys. Res. Lett.*, *32*, L23710, doi:10.1029/2005GL024368.

Schmittner, A., T. A. M. Silva, K. Fraedrich, E. Kirk, and F. Lunkeit (2011), Effects of mountains and ice sheets on global ocean circulation, *J. Clim.*, *24*, 2814–2829, doi:10.1175/2010JCLI3982.1.

Stocker, T. F., D. Qin, G.-K. Plattner, M. Tignor, S. K. Allen, J. Boschung, A. Nauels, Y. Xia, V. Bex, and P. M. Midgley (eds.) (2013), Climate Change 2013: The Physical Science Basis. Contribution of Working Group I to the Fifth Assessment Report of the Intergovernmental Panel on Climate Change, 1535 pp., Cambridge Univ. Press, Cambridge, U. K., and New York, doi:10.1017/CBO9781107415324.

Stocker, T. F., Q. Dahe, and G. Plattner (2013), *Working Group I Contribution to the IPCC Fifth Assessment Report (Ar5), Climate Change 2013: The Physical Science Basis*, Geneva, Switzerland.

Stommel, H. M. (1961), Thermohaline convection with two stable regimes of flow, *Tellus*, *13*(2), 224–230, doi:10.1111/j.2153-3490.1961.tb00079.x.

Stouffer, R. J., et al. (2006), Investigating the causes of the response of the thermohaline circulation to past and future climate changes, *J. Clim.*, *19*(8), 1365–1387, doi:10.1175/JCLI3689.1.

Swingedouw, D., C. B. Rodehacke, S. M. Olsen, M. Menary, Y. Gao, U. Mikolajewicz, and J. Mignot (2015), On the reduced sensitivity of the Atlantic overturning to Greenland ice sheet melting in projections: A multi-model assessment, *Clim. Dyn.*, *44*(11–12), 3261–3279, doi:10.1007/s00382-014-2270-x.

van den Berk, J., and S. S. Drijfhout (2014), A realistic freshwater forcing protocol for ocean-coupled climate models, *Ocean Model.*, *81*, 36–48, doi:10.1016/j.ocemod.2014.07.003.

van den Broeke, M. R., E. M. Enderlin, I. M. Howat, P. Kuipers Munneke, B. P. Y. Noel, W. J. van den Berg, E. van Meijgaard, and B. Wouters (2016), On the recent contribution of the Greenland ice sheet to sea level change, *Cryosphere*, *10*, 1933–1946, doi:10.5194/tc-10-1933-2016.

Weijer, W., M. E. Maltrud, M. W. Hecht, H. A. Dijkstra, and M. A. Kliphuis (2012), Response of the Atlantic Ocean circulation to Greenland Ice Sheet melting in a strongly-eddying ocean model, *Geophys. Res. Lett.*, *39*, L09606, doi:10.1029/2012GL051611.

Wouters, B., D. Chambers, and E. J. O. Schrama (2008), GRACE observes small-scale mass loss in Greenland, *Geophys. Res. Lett.*, *35*, L20501, doi:10.1029/2008GL034816.

Yang, D., and O. A. Saenko (2012), Ocean heat transport and its projected change in CanESM2, *J. Clim.*, *25*, 8148–8163, doi:10.1175/JCLI-D-11-00715.1.

Zickfeld, K., T. Slawig, and S. Rahmstorf (2004), A low-order model for the response of the Atlantic thermohaline circulation to climate change, *Ocean Dyn.*, *54*(1), 8–26, doi:10.1007/s10236-003-0054-7.